X-625-77-135
PREPRINT

TMX-71334

OBSERVATIONS OF LARGE TRANSIENT MAGNETOSPHERIC ELECTRIC FIELDS

T. L. AGGSON
J. P. HEPPNER

MARCH 1977

GSFC
GODDARD SPACE FLIGHT CENTER
GREENBELT, MARYLAND

OBSERVATIONS OF LARGE TRANSIENT MAGNETOSPHERIC ELECTRIC FIELDS

T. L. Aggson
J. P. Heppner

MARCH 1977

ABSTRACT

Transient electric field events have been observed with the long, double probe instrumentation carried by the IMP-6 satellite. Nine, clearly defined, exceptionally large amplitude events are presented here. The events are observed in the midnight sector at geocentric distances 3.5 to 5.5 R_e at middle latitudes within a magnetic L-shell range of 4.8 to 7.5. They usually have a total duration of one to several minutes with peak power spectra amplitudes occurring at a frequency of about 0.3 Hz. The events occur under magnetically disturbed conditions and in most cases they can be associated with negative dH/dt excursions at magnetic observatories located near the foot of the magnetic field line intersecting IMP-6. These electric field events should cause violation of the second and third magnetic adiabatic invariants for the proton population and should violate all three invariants for the heavier ion populations. The magnetospheric motions calculated for these electric fields indicate a quasi-stochastical diffusive process rather than the general inward magnetospheric collapsing motion expected during the expansive phases of auroral substorm activity. The transient electric fields provide an obvious mechanism for the impulsive acceleration and injection of plasma to populate the outer radiation belt.

INTRODUCTION

The role of time dependent electric fields in the acceleration and injection of hot plasma to form the outer radiation belt was initially discussed by Gold (1959) and Kellog (1959). Konradi (1967), using Explorer 12 data, and the University of Minnesota experimenters (Parks and Winckler, 1968; Pfitzer and Winckler, 1969; Arnoldy and Chan, 1969; Lezniak and Winckler, 1970), using data from ATS-1 and OGO-3, clearly showed that energetic particles are impulsively injected into the magnetosphere in the midnight sector at equatorial L-values that project into the nightside auroral belt. They also showed that these injections were closely associated with the appearance of magnetic bays (i.e., substorm enhancements) in the nightside auroral belt. The ATS-5 observations of DeForest and McIlwain (1971) extended the measurements to low energies (50 ev to 50 kev) and a one-to-one correspondence between injection events and magnetic bay enhancements was found in many cases.

Based on the above observations and more numerous observations of the dynamic behavior of plasmas and magnetic fields in more distant tail regions, models and mechanisms for explaining the injections and substorm associations have been the subject of a large number of papers. In general, the complexity of the problem becomes over simplified in theoretical treatments which tend to assume that there are direct cause and effect relationships between phenomena that are statistically correlated. Several recent papers indicate the complexity. For examples: Rostoker et al. (1975) argue that the correlations with energetic particle injections at synchronous altitudes depend on a spatial association with the poleward boundary of the substorm-intensified westward electrojet,

and Lui et al. (1975) find numerous exceptions to often quoted statistical relationships between the interplanetary magnetic field and the plasma sheet dynamics associated with substorms.

The role of electric fields in the acceleration and injection process has been observationally unknown although it is a key factor in many, but not all, mechanisms. The observations reported here do not totally define that role, or provide proof that intense transient electric fields are the only cause of sudden particle acceleration and injection. They do, however, demonstrate that such fields exist. The location of the region where strong E-field transients have been observed, in the midnight sector between L=4.8 and 7.5, and the frequent association with -dH/dt transients near the foot of the IMP-6 magnetic field line, also suggest that these events are likely to be associated with the particle accelerations and injections observed by spacecraft in synchronous orbits. The purpose of this paper is to describe these large amplitude E-field events and to illustrate their correlation with magnetic substorm activity.

MEASUREMENT LIMITATIONS

As demonstrated by sounding rocket experiments, low altitude satellite measurements, and measurements inside the plasmapause from satellites in highly eccentric orbits, the symmetric double probe, floating potential technique provides accurate measurements of the ambient electric field in dense (e.g., $\geq 10^3$ el/cm^3) plasmas with relatively small (e.g., 10 to 20 meter) probe separations. Beginning with OGO-5, it has also become well known (e.g., review by Heppner, 1972a) that in low (e.g., $\leq 10^2$ el/cm^3) density plasmas the sheath surrounding the spacecraft drastically changes characteristics and increases dimensions. The consequence is not only an undesirable interaction between the sheath plasma and the probes, but also the fact that this interaction is sensitive to density and temperature changes in the ambient plasma which affect the sheath characteristics. Thus, a variation in an ambient parameter, such as plasma density, can appear as a variation in the electric field even though the actual electric field is zero or constant.

Without going into the complexities of the sheath interaction here, the fact that it is complex can be appreciated by noting that it is not a simple function of the spacecraft potential. For example, the observations indicate that the sheath does not necessarily collapse when the spacecraft potential is close to, or passes through zero. Thus, control of the potential does not provide a solution and the only known solution at present is to increase the probe separation. Limits are not known but extrapolations suggest that probe separations of about 200 meters are needed to obtain accurate measurements over large portions of the magneto-sphere.

IMP-6 carried 3 pairs of long cylindrical (1.25 cm., diameter) antenna probes which were deployed to different distances. The effective electric field baseline separations (the distance between midpoints of the conducting tip sections) were calibrated during perigee passes to be 35 and 67 meters, respectively, along the spacecraft x and y axes in the spin plane, and 6 meters along the spin, z, axis. The calibration comes from the measurement of $\underline{v} \times \underline{B}$ where $\underline{v}$ is the satellite velocity and $\underline{B}$ is a model magnetic field. Under average conditions the 6 meter measurements are only meaningful near perigee and the 35 meter measurements are obscured by sheath effects throughout most of the magnetosphere; noise levels of the order of 1 mv/m are common but they are also observed as low as 0.3 mv/m. Extremely large (e.g., up to 100 mv/m) sheath signals, similar to those observed with the 35 meter probes, are also frequently observed. As the expected magnetospheric fields, in the range 0.1 to 1 mv/m, are comparable to noise levels, it is difficult to determine the validity and accuracy of the DC measurements even under favorable conditions for these weak fields.

It is important to recognize that the detection and analysis of the events reported here is not compromised by the above limitations. The sudden occurrence and magnitudes of these events simplify detection. Most important, however, is that the electric field intensities observed by the 35 meter probes agree with the 67 meter measurements, and in some cases this agreement also appears to extend to the short, 6 meter probes. This is the opposite of a sheath effect where the quantity $E = \Delta V/d$ becomes large for small probe separations because of both the smaller value of d (the probe separation) and the larger magnitude of ΔV (the difference in potential between the two probes) when the ΔV is from

sheath potentials.

In addition to measurements of $\Delta V = V_1 - V_2$ for each axis, the common mode voltage $(V_1 - V_0)$, where V_0 is the spacecraft reference potential, is measured for one probe along each axis. An AC coupled frequency spectrometer also provides both peak and rms measurements in 12 frequency bands between 0.1 and 100 Hz. By ground command it was possible to assign the spectrometer to any one of the three axes; however, for the events reported here it was always assigned to the y (67 meter) axis.

OBSERVATIONS

IMP-6 was placed in an eccentric earth orbit with an orbital period of about 4 days. The satellite typically is within auroral belt L-shells in dipole representations for only a few hours per orbit along in- and out-bound passes. Events of the type reported here are seen only on a small fraction of the total number of orbits and their duration, when seen, is limited to a small fraction of the time spent on auroral belt L-shells. Occurrences also appear to be limited to the nightside of the earth.

Figures 1 and 2 (a, b, c, and d) illustrate one event in detail. Figure 1 shows: the X and Y components of $\underline{E}$ in solar-ecliptic coordinates, the common voltage ($V_{-y} - V_o$) which is the voltage between the probe on the -y axis and spacecraft ground, the rms voltage in the 45-100 Hz band plotted on a log-compressed scale, and the peak value of the electric field in the 0.1 - 0.18 Hz band also plotted on a log-compressed scale. The DC field in solar-ecliptic coordinates comes from a least squares sine wave fit to the spin modulated electric field that appears on the 67 meter axis. The actual maximum electric field was coherent for only about 5 seconds at 22:35 UT and is thus somewhat filtered out in fitting to the 11 second periodicity of the satellite spin. The slope of the straight line placed on Figure 2(a), roughly 114 mv/m, is more indicative of the maximum field for this event. (Note: as the spacecraft spin axis was within a few degrees of being normal to the solar-ecliptic plane, measurements in the spin plane are treated as being in the solar-ecliptic plane).

Figure 2(a) shows the maximum voltage difference between the two probes on each axis for all three axes as a function of the distance between probes on each axis. Deviation from a single value for $E=\Delta V/d$ for the two axes in the spin plane is a consequence of the length of the spin period and the short duration of the peak field. However, the crude agreement, plus the fact that ΔV for 67 meters is much greater than ΔV at 35 meters, illustrates that this is not a sheath effect as discussed earlier. The lack of change in the common mode voltage, Figure 1, also indicates that the measurements are not related to any unusual spacecraft charging of the type reported by DeForest (1972) for vehicles in synchronous orbits.

In Figure 2(b) the maximum voltage difference in each of 16 azimuth sectors taken from instantaneous samples at the sampling rate of 1.56 samples/sec, is shown for the 67 meter probes. Figure 2(c) illustrates the peak voltage difference as a function of frequency by combining the spectrometer measurements above 0.1 Hz and the least squares fit for lower frequencies. Figure 2(d) gives the magnitude and direction of $\underline{E}$ in the solar-ecliptic plane, based on the 11 second fit, for a more extended period of time. Particularly from two to ten minutes following the event a fluctuating, 1 to 8 mv/m, field is indicated. Although these weaker fields are not unreasonably high relative to possible convective field strengths that might be anticipated, one cannot accurately determine the fractional influence of noise from the spacecraft sheath.

The two features which characterize the event on orbit 203, and the 8 other events discussed here, are the transitory nature of the event and

the large amplitude. The nine events with these similar characteristics are tabulated in Table 1. From the locations listed it is apparent that observations of the events can also be characterized as occurring within a very limited region of the magnetosphere: in particular, within 2 hours of magnetic midnight between dipole L-values 4.8 and 7.5. The observations also divide into two groups defined by a restricted range of + and - geomagnetic latitudes; this is a seasonal orbit effect that separates the observations made on inbound and outbound passes. It further implies that if such events, in general, only occur on auroral L-shells near midnight, they can only be observed by IMP-6 when IMP-6 is in the summer hemisphere (Note: the spatial clustering of the events is also illustrated in Figure 11, discussed later).

As a first step toward understanding these transients it is important to establish whether they are essentially temporal variations or instead the result of the satellite crossing spatial regions of different electrostatic potential. It is well known from measurements and observations that the midnight region of the magnetosphere at L>5 undergoes sudden aperiodic changes which correlate with auroral substorm enhancements that are similarly highly temporal. On the other hand there are theoretical models which predict the existence of electrostatic boundary layers such as the Alfvén layers in Jaggi and Wolf's (1973) model or Swift's (1975) model for the acceleration of auroral electrons by steady state oblique electrostatic shocks.

To determine the relative likelihood of the electric field transients being spatial or temporal, simultaneous high latitude magnetograms were examined extensively. The results from this correlative study, given in the next section, clearly favor the temporal interpretation and thus

description as "events". Interpretation in terms of a persistent spatial structure appears highly unlikely from the standpoint that there are many satellite passes when transients are not observed. It should, of course, be recognized that the temporal occurrence is spatially confined to a limited region of the magnetosphere and further that one does not know that the duration of the event is the same throughout that region.

CORRELATION WITH AURORAL SUBSTORM ACTIVITY

It is often difficult to define the exact onset time of a substorm enhancement in the auroral region from ground station magnetograms. This is due in part to the paucity of ground station coverage and the complexity of variations accompanying an onset when stations are displaced from the onset location. Considered locally in the auroral belt the sudden onset of a negative bay occurs (a) at the time of auroral break-up, (b) at the time the eastward ionospheric current previously associated with the lowest latitude auroral arcs is disrupted in the break-up region, (c) with a large increase, following this time, of the westward current cross'ng the meridian of the onset, and (d) with the reversal of the east-west direction of auroral motions. These dynamic changes are characteristically described as sudden temporal variations at the Harang discontinuity (see, e.g., Heppner, 1972b). To avoid the complexities of identifying substorm onsets from auroral belt stations several investigators (see, e.g., McPherron et al., 1973) have selected onset times from middle latitude positive bays that accompany some substorms with a recognizeable signature. However, as many substorm enhancements, including cases of large amplitude, are not readily identifiable at middle latitudes, this approach misses many events. The approach taken here, relative to a limited number of magnetospheric events, has thus been one of using all the data available from high latitude magnetic observatories.

The apparent association of each event with surface magnetic field transients is summarized in Table 2. This is a condensation in the sense that the surface transients are in some cases seen by more stations than those listed; in these cases the listed stations are representative but

the listing is not comprehensive. Table 3 provides a list of the observatories routinely examined, with an identification of the abbreviations used in Table 2. Through use of the columns "magnetic local time" in Table 1 and "UT of local magnetic midnight" in Table 3 one can also readily estimate the local time proximity of the transients in Table 2 and the electric field events in Table 1. In most cases it is apparent that the event is associated with transients occuring at the station(s) closest to the northern foot (or sub-conjugate point) of the field line passing through IMP-6.

Columns 2, 3, and 4 of Table 2 are not independent. All three express the existence of large transient variations in space-time proximity to the Harang discontinuity and substorm enhancements at the time of an event at IMP-6. The separation into 3 columns merely avoids the need for a precise definition of a substorm onset. For example, in Event 179 (actually two events beginning at 08:40 and 08:47, Table 1) large transients first appeared in the Alaska sector at 08:38 but with subsequent large excursions involving changes in the sign of the H-component it would not be precise in terms of common practice to call this an onset time. Thus, the associated surface transients are noted in column 2 rather than 3. Event 199 is a more complicated example in that the bay "onset" at Meanook occurred superimposed on an existing $-\Delta H$ during a period of transient (+ and -) excursions in H in the Alaska sector.

An important point illustrated by Table 2 is that all nine events occur in association with surface transients. In 7 of the 9 cases the surface transients occur in space-time association with the Harang discontinuity and/or substorm enhancements. Of the remaining two, one event

(186) occurs at IMP-6 in the post-midnight region during the course of a large substorm but correlated transients are seen over a broad region as illustrated later in Figure 4. The other exception in Table 2 is Event 165 (05:05 UT in Table 1) which represents the weakest case for demonstrating the correlation with surface transients. In this case there is a sharp transient in the D and Z magnetic components from 05:00 to 05:03 UT at the closest sub-conjugate observatory (Great Whale) but the variation in H does not make it clear that this is a substorm onset. As other observatories, with the exception of Baker Lake, do not show a transient at this time, this case suggests that the correlation between the electric field events and surface activity can on occasion be localized to a relatively small flux tube cross-section.

To more clearly illustrate the correlations tabulated in Table 2, magnetograms from groups of observatories are shown for three events in Figures 3, 4, and 5. To further illustrate the close time relationships, both in UT and magnetic local time, Figures 6, 7, 8 and 9 show magnetograms from stations near the sub-conjugate point on an expanded time scale for four additional events.

The Figure 3 magnetograms clearly show the onset of a negative bay disturbance in the sub-conjugate Scandinavian sector several minutes prior to the electric field Event 203 which is illustrated in detail in Figures 1 and 2. The UT time difference is similar to the time difference previously found between bay onsets and magnetic field collapse event observed by OGO-I (Heppner et al., 1967) in near-tail regions.

Figure 4 illustrates the somewhat anomolous Event 186 where the sub-conjugate point lies in the post-midnight bay region. In this case the

Harang discontinuity lies to the west of College, Alaska in a region where data are not available. However, a simultaneous magnetic field transient is obvious at all middle latitude nightside observatories and a simultaneous sharp spike appears at the Tixie Bay and Dixon Island observatories in the evening auroral belt. The correlated surface transient is thus more widespread than in most cases.

Figure 5 presents a case, Event 209, in which an exceptionally sharp and large amplitude spike preceded the first of two electric field transients. Because of the faint trace on the Kiruna magnetogram, caused by the transient excursion, the exact magnitude of the change may be somewhat questionable. Existence, and natural cause, is confirmed by the simultaneous gap at Sodankyla and the smaller spike at Abisko. The second event appears following a smaller transient at Murmansk which is not apparent in the other Scandinavian stations. Further to the west there was an abrupt negative bay onset at Syowa in the southern hemisphere (not shown) simultaneous with the second Murmansk transient (Note: Syowa is approximately conjugate to the Leirvogur observatory where data were not available for this event).

Figures 6, 7, 8 and 9 illustrate Events 168, 172, 199 and 249, respectively, on an expanded scale. The magnetic field records in Figures 6, 7 and 8 are from the observatory closest to the sub-conjugate foot of the magnetic field line passing through IMP-6. In the two cases (Events 172 and 199) where this was Meanook, large transient variations were also present at earlier magnetic local times in Alaska as indicated in Table 2. Event 249, Figure 9, was associated with a surface transient over a somewhat greater range of longitudes and magnetic local time. Data from the Bear Island station, located to the north of the listed Scandinavian

stations, were available for this event. The principal transient at Bear Island and Dixon, at a later magnetic local time, was a $-\Delta H$ excursion whereas the principal response at Scandinavian stations closest to the sub-conjugate point was a $+\Delta H$ change immediately prior to the electric field event at 19:17. This is illustrated in Figure 10.

Inasmuch as all nine events are clearly associated with the occurrence of magnetic field transients in the surface region intersected by magnetic field lines passing through IMP-6, the electric field events are logically interpreted to be temporal variations. It does not, however, necessarily follow that similar electric field events are present whenever there is a magnetic field transient at the earth's surface. As illustrated by the examples shown, the correlated surface transients in some cases are distributed over wide sections of the earth and in other cases they appear to be regionally confined to a relatively small sub-conjugate area. Most typically, the beginning of the surface transients precedes or is simultaneous with the satellite event. Particularly when the surface transient precedes the satellite event the possibility exists that the event has a total duration which is longer than that observed at the location of IMP-6 because the spatial dimensions at any instant of time are not accurately known. However, it is unlikely that IMP-6 simply passes through a standing localized structure inasmuch as the satellite velocity is roughly two orders of magnitude less than the transient drift velocity, $\underline{E}(t) \times \underline{B}/B^2$. Multiple satellites would be required to determine the spatial dimensions as a detailed function of time throughout an event. Relative to possible interpretations of the electric field events it is important to note that polar cap magnetograms were also examined and they did not reveal any close correla-

tions. Indications of possible correlation were in fact too questionable to include in Table 2.

MAGNETOSPHERIC MOTION

It has been recognized for sometime that accompanying the onset of an auroral substorm enhancement there are large scale changes in the magnetosphere in the midnight sector which suggest that the tail field is collapsing inward toward the earth. The collapse is frequently attributed to a decrease in the neutral sheet current. Radial penetration and injection of hot plasma is also frequently attributed to the earthward, collapsing motion. Prior to critical examination, the transients described here were also presented (Aggson and Heppner, 1976) with the view that they could probably be attributed to the collapse phenomena. However, as described below, subsequent analyses have not supported this view.

The change in magnetic field geometry accompanying a collapse in the midnight sector has been illustrated by Lezniak and Winckler (1970). Using their geometry it is apparent from $\underline{E} = -(\underline{v} \times \underline{B})$ that the inward velocity, $\underline{v}$, should give a westward electric field. At midnight this is a + Y electric field in solar-ecliptic coordinates. Similarly, from the change in the volume integral of the current density (i.e., the time derivative of the magnetic vector potential) it is apparent that the inductive electric field on the earthward side of a decaying neutral sheet current is also westward in the midnight sector.

The observed electric field transients are to a first approximation quasi-oscillatory (e.g., Figures 1 and 2). However, one can relate the time integral of the transient to convective magnetospheric motions. For this purpose a model magnetic field is used because the ambient magnetic field is greater than the saturation level of the IMP-6 magnetometer in most cases. As the orbit is such that events are observed only in the

summer hemisphere, a tilted magnetic dipole model is most applicable. Figure 11, based on a tilt model from Mead and Fairfield (1975), illustrates the field geometry at the event locations. For simplicity, the events observed in the southern, summer hemisphere are shown at equivalent northern, summer hemisphere locations. It is apparent from Figure 11 that the magnetic field vector is approximately in the +X solar-ecliptic direction for events near midnight. Thus, as shown in detail by Lezniak and Winckler (1970), a magnetospheric collapse will produce a -Z flux tube motion in solar-ecliptic coordinates at the IMP-6 locations. The combination $-v_z$ and B_x at these locations is, of course, equivalent to the combination v_x and B_z at the equator in producing a $+E_y$ electric field during a collapse.

Lack of agreement between the observed events and the simple collapse picture above is illustrated by Event 203 presented in Figures 1 and 2. The algebraic sum of the 11 second averages over the 5 minute duration of Event 203 gives $\int E_y dt = -238 \pm 50$ volts/km/sec. Thus, the average Y component of the electric field during the event is negative rather than positive. This corresponds to a modest outward movement over a distance $\Delta s = 600 \pm 126$ km from $\Delta s = v.dt$ using model values for $\underline{B}$ to calculate $\underline{v} = (\underline{E} \times \underline{B})/B^2$ for the Y component of $\underline{E}$.

Event 203 is typical of the other eight events in the sense of not providing any evidence of statistically significant inward motion. The maximum electric fields observed during these events are oscillatory in appearance with a maximum in the power spectra occurring near 0.3 Hz. The 11 second averages appear to be quasi-stochastic and taken as an ensemble the time averaged electric fields of the 9 events appear to be random in polarity. Thus, association of the transient electric fields

with localized plasma instabilities seems more likely than association with a large scale magnetospheric collapsing motion.

PARTICLE INJECTION BY DIFFUSION

Except for the quasi-oscillatory nature of the electric field events, their magnitudes and morphological association with substorm enhancements are such that they are obvious candidates for explaining the impulsive acceleration and injection of trapped particles frequently observed by satellites in synchronous orbits. Thus it is appropriate here to briefly consider the diffusion of particles transverse to the magnetic field. Event 203, Figures 1 and 2, is again illustrative.

The local ion gyrofrequency for protons for Event 203 is approximately 6 Hz. As shown by Figure 2 (c), this frequency is more than an order of magnitude greater than the frequency where peak voltages occur. Thus appreciable ion cyclotron scattering of protons is questionable. The local ion gyrofrequency for singly charged oxygen is, however, very close to the frequency of peak voltage. In light of recent measurements by Shelley et al., (1976) showing a large flux of O^+ flowing away from the auroral ionosphere it is appropriate to look further at the scattering of O^+. Assuming that the electric fields are essentially stochastic one can apply the simple equations of Puri (1966) to estimate the transverse diffusion. His eq. 24 reads:

$$d\langle x^2\rangle/dt = \pi/B_o^2 [\Phi(\omega_c) + 2\Phi(\omega=0)]$$

where the first term represents the scattering at the ion gyrofrequency and the second term is in agreement with Spitzer's (1960) derivation of Bohm diffusion. Here Φ is the power spectra of the random electric field. More comprehensive calculations of radial diffusion from ion cyclotron scattering are available (e.g., Schulz and Lanzerotti, 1974;

Sturrock, 1966); however, these involve the momentum spectra of the particles and are beyond the scopc of consideration here. Using the above equation for 0^+ and the frequency spectra of Figure 2(c), a mean scattering distance of about 2000 km is obtained for Event 203. Application of the above equation for Bohm scattering is considerably more subtle. For a rough approximation one can estimate the power spectra at $\omega = 0$ from the time average of all nine events as an ensemble. Although sensitive to errors this gives a mean scattering distance of the order 1000 km which is also applicable to protons. Thus, these strong scattering processes appear capable of injecting particles in the outer radiation belt and they appear to be an attractive alternative to injection by convective collapse which we have not observed.

DISCUSSION

The existence of transient electric field events of the type reported here has a bearing on many previously reported magnetospheric observations. These are too numerous for discussion; however, several observations which are particularly current should be mentioned in terms of the likelihood of a close association.

1. Gurnett and Frank (1977) have reported intense plasma wave turbulence between 10 Hz and several kHz on auroral belt field lines. This turbulence is found along an essentially continuous band of auroral L-shells at all local times. Maximum electric field strengths of about 10 millivolts/ meter are observed between 10 and 50 Hz. Although this type of signal is often seen for durations up to 5 minutes before and after the large transient electric field events (e.g., the 54 - 100 Hz band in Figure 1), the spectra reported by Gurnett and Frank is generally at an order of magnitude higher frequency and amplitudes are an order of magnitude lower than those observed during the events reported here.

2. Mozer et al. (1977) have reported the existence of very narrow regions of large electric fields in the auroral zone at altitudes below 8000 km. The fields are interpreted in terms of a spatial shock structure believed to be associated with relatively stable auroral arcs in the ionosphere. There is not any evidence that these lower altitude observations can be related to the transient events reported here. The events reported here are associated with highly transient changes in the auroral ionosphere and are thus believed to be highly transient in existence.

3. Sarris et al. (1976) observed magnetospheric bursts of high energy protons and electrons at 35 R_e on IMP-7. From examination of data

from a similar experiment on IMP-6, Sarris (personal communication) found that the electric field transients described here were coincident with particle bursts at energies similar to those reported for IMP-7.

4. Fairfield (1973) identified magnetic field signatures of substorms on high latitude field lines in the nighttime magnetosphere. In two cases where the IMP-6 magnetometer was not saturated Fairfield (personal communication) found similar signatures coincident with the transient events reported here. The magnetic field change, of the order 10 gammas, suggests that a change in the field-aligned current accompanies the electric field transients.

The main purpose in this paper has been to report the existence of the electric field transients and their correlation with substorm transients as observed at the earth's surface. The correlations clearly suggest that the cause of the electric field transients should be related on an almost one to one basis with the cause of the auroral break-up, substorm enhancement phenomena. A number of both microscopic and macroscopic instabilities associated with field-aligned currents appear in the literature. From the standpoint that field-aligned current enhancements are likely to accompany auroral break-up phenomena, it is possible that one of these instabilities may provide a mechanism for creating the electric field transients. These possibilities are not evaluated here. Quantitative correlation with simultaneous particle measurements will in future analyses provide a more comprehensive basis for discussing cause and effect mechanisms.

Aggson, T. L. and J. P. Heppner, Observations of large transient magnetospheric electric fields, EOS, 57, 317, 1976.

Arnoldy, R. L. and K. W. Chan, Particle substorms observed at the geostationary orbit, J. Geophys. Res., 74, 5019, 1969.

DeForest, S. E. and C. E. McIlwain, Plasma clouds in the magnetosphere, J. Geophys. Res., 76, 3587, 1971.

DeForest, S. E., Spacecraft charging at synchronous orbit, J. Geophys. Res., 77, 651, 1972.

Fairfield, D. H., Magnetic field signatures of substorms on high latitude field lines in the nighttime magnetosphere, J. Geophys. Res., 78, 1553, 1973.

Gold, T., Origin of the radiation near the earth discovered by means of satellites, Nature, 183, 355, 1959.

Gurnett, D. A. and L. A. Frank, A region of intense plasma wave turbulence on auroral field lines, J. Geophys. Res., 82, 1031, 1977.

Heppner, J. P., M. Sugiura, T. L. Skillman, B. G. Ledley, and M. Campbell, OGO-A Magnetic field observations, J. Geophys. Res., 72, 5417, 1967.

Heppner, J. P., Electric fields in the magnetosphere, in Critical Problems of Magnetospheric Physics, ed. by E. R. Dyer, p. 107, Nat. Acad. of Sci., Washington, DC, 1972a.

Heppner, J. P., The Harang discontinuity in auroral belt ionospheric currents, Geofysiska Publikasjoner, 29, 105, 1972b.

Jaggi, R. K. and R. A. Wolf, Self-consistent calculation of the motion of a sheet of ions in the magnetosphere, J. Geophys. Res., 78, 2852, 1973.

Kellog, P. J., Van Allen radiation of solar origin, Nature, 183, 1295, 1959.

Konradi, A., Proton events in the magnetosphere associated with magnetic bays, J. Geophys. Res., 72, 3829, 1967.

Lezniak, T. W and J. R. Winckler, Experimental study of magnetospheric motions and the acceleration of energetic electrons during substorms, J. Geophys. Res., 75, 7075, 1970.

'ui, A. T. Y., E. W. Hones, D. Venkatesan, S.-I. Akasofu, and S. J. Bame, Response of the plasma sheet at 18 Re to sudden southward turnings of the interplanetary magnetic field, J. Geophys. Res., 80, 929, 1975.

McPherron, R. L., C. T. Russell, M. G. Kivelson, and P. J. Coleman, Jr., Substorms in space: The correlation between ground and satellite observations of the magnetic field, Radio Sci., 8, 1059, 1973

Mead, G. D. and D. H. Fairfield, A quantitative magnetospheric model derived from spacecraft magnetometer data, J. Geophys. Res., 80, 523, 1975.

Mozer, F. S., C. W. Carlson, M. K. Hudson, R. B. Torbert, B. Parady, J. Yatteau, and M. C. Kelley, Observations of paired electrostatic shocks in the polar magnetosphere, Phys. Rev. Letrs., to be published, 1977.

Parks, G. K. and J. R. Winckler, Acceleration of energetic electrons observed at synchronous altitude during magnetospheric substorms, J. Geophys. Res., 73, 5786, 1968.

Pfitzer, K. A. and J. R. Winckler, Intensity correlations and substorm electron drift effects in the outer radiation belt measured with the OGO-3 and ATS-1 satellites, J. Geophys. Res., 74, 5005, 1969.

Puri, S., Plasma heating and diffusion in stochastic fields, Phys. Fluids, 9, 2043, 1966.

Rostoker, G., J. L. Kisabeth, R. D Sharp, and E. G. Shelley, The expansive phase of magnetospheric substorms 2. The response at synchronous altitude of particles of different energy ranges, J. Geophys. Res., 80, 3557, 1975.

Sarris, E. T., S. M. Krimigis, and T. P. Armstrong, Observations of magnetospheric bursts of high-energy protons and electrons at 35 R_e with IMP-7 J. Geophys. Res., 81, 2341, 1976.

Shelley, E. G., R. D. Sharp, and R. G. Johnson, Satellite observations of an ionospheric acceleration mechanism, Geophys. Res. Ltrs., 3, 654, 1976.

Spitzer, L. Jr., Particle diffusion across a magnetic field, Phys. Fluids, 3, 659, 1960.

Schulz, M. and L. J. Lanzerotti, Particle diffusion in the radiation belts pp. 96-98, Springer-Verlag, New York, 1974.

Sturrock, P. A., Stochastical acceleration, Phys. Rev., 141, 186, 1966.

Swift, D. W., On the formation of auroral arcs and acceleration of auroral electrons, J. Geophys. Res., 80, 2096, 1975.

FIGURE CAPTIONS

Figure 1: Electric field measurements of a transient magnetospheric event.

Figure 2(a): Event 203, peak voltage difference as a function of the 3 double probe separations.

Figure 2(b): Event 203, peak voltage difference as a function of solar-ecliptic azimuth for the 67 meter probes.

Figure 2(c): Event 203, peak voltage difference as a function of frequency for the 67 meter probes.

Figure 2(d): Event 203, amplitude and phase of the DC electric field as a function of time for 67 meter probes.

Figure 3: Magnetograms from the region sub-conjugate to IMP-6 at the time of Event 203.

Figure 4: Event 186 (upper left) and simultaneous surface magnetograms.

Figure 5: Event 209 (upper left) and simultaneous surface magnetograms.

Figure 6: Event 168 and a sub-conjugate surface magnetic record.

Figure 7: Event 172 and a sub-conjugate surface magnetic record.

Figure 8: Event 199 and a sub-conjugate surface magnetic record.

Figure 9: Event 249 and a surface magnetic record to the north of the sub-conjugate region.

Figure 10: Surface magnetic records encompassing the time of Event 249.

Figure 11: Meridional view of the locations of the 9 events compared with a Meak-Fairfield (1975) magnetic field model. Events which occurred in the southern, summer hemisphere are shown at equivalent locations in the northern, summer hemesphere.

Table 1: Times and Locations of Large Amplitude E-Field Events

Event (orbit) Number	Date	UT*	Geocentric Distance (km)	Geomagnetic Longitude	Geomagnetic Latitude	Magnetic Local Time	L
165	1-26-73	5:05	35175.	-30°	-28.7°	22:24	7.16
168	2- 7-73	17:03	31250.	-163°	-40.5°	1:36	5.70
172	2-24-73	6:53	26669.	-54°	-33.0°	22:36	5.94
179	3-25-73	8:40	22815.	-90°	-36.7°	21:54	5.56
		8:47	21730.	-86°	-33.0°	22:12	4.82
186	4-19-73	8:41	22420.	-33°	38.5°	1:42	5.74
199	6-12-73	7:51	25059.	-61°	39.5°	23:00	6.61
		7:58	26279.	-57°	41.5°	23:12	7.34
203	6-28-73	22:34	32569.	104°	34.4°	1:18	7.49
209	7-23-73	19:29	26896.	112°	31.7°	22:30	5.82
		19:40	28928.	116°	31.9°	23:07	6.28
249	1- 9-74	19:17	26691.	131°	-39.6°	23:18	7.05

*Beginning of event as seen in the 0.1 - 0.18 Hz band

Table 2: Apparent Associations with Surface Magnetic Activity

Event (orbit) Number	with large variations near the Harang discontinuity	with sudden substorm enhancements (onsets ?) of bays	with other auroral belt transients			with sudden changes at lower latitudes	3-hour K_p
			during -dH/dt phase of bay	during phase of maximum disturbance	not readily classified by substorm phase		
165					GW, BL(?)		3+
168		17:03 DI, TX				Central Asia (?)	3+
172	CO, SI	(D) 06:51 SI (Z) 07:00 SI (H) 07:00+ CO	ME				5+
179	BA, CO, SI						5
186				ME, WE, and Alaska sector	Spike oscillation DI & TX	All mid.lat. nightside stations	5-
199	BA, CO	08:00 ME	ME				3+
203		(H) 22:24 TR (D) 22:30 MM (D) 22:34 SO	European sector			All longitudes	5
209		19:25-19:26 TR, AB, MM, SO, KI	European sector				3-
		19:38 Syowa(*)	19:38 MM		19:41 NQ		
249		19:11 DI			19:11 TX 19:11-19:17 European sector		2+

(?) Questionable inclusion in Table

(*) Conjugate substitute for missing LR data

Table 3: Auroral Belt Observatories Examined for Table 2

	Name	L	UT of Local Magnetic Midnight
(NQ)	Narssarssuaq	7.0	02:07
(GW)	Great Whale	6.7	05:25
(CH)	Churchill	8.6	07:03
(BL)	Baker Lake	14.9	07:33
(ME)	Meanook	4.7	08:32
(SI)	Sitka	3.9	10:17
(CO)	College	5.5	11:34
(BA)	Barrow	8.1	12:19
(WE)	Cape Wellen	4.6	12:53
(TX)	Tixie Bay	5.6	15:53
(CC)	*Cape Chelyuskin	9.5	16:51
(DI)	Dixon Island	6.9	17:59
(MM)	Murmansk	5.2	20:09
(SO)	Sodankyla	5.1	20:32
(TR)	Tromso	6.2	20:46
(AB)	Abisko	5.6	20:53
(KI)	Kiruna	5.3	21:00
(LE)	Lerwick	3.7	22:49
(LR)	*Leirvogur	6.0	23:50

*Data available for only some events

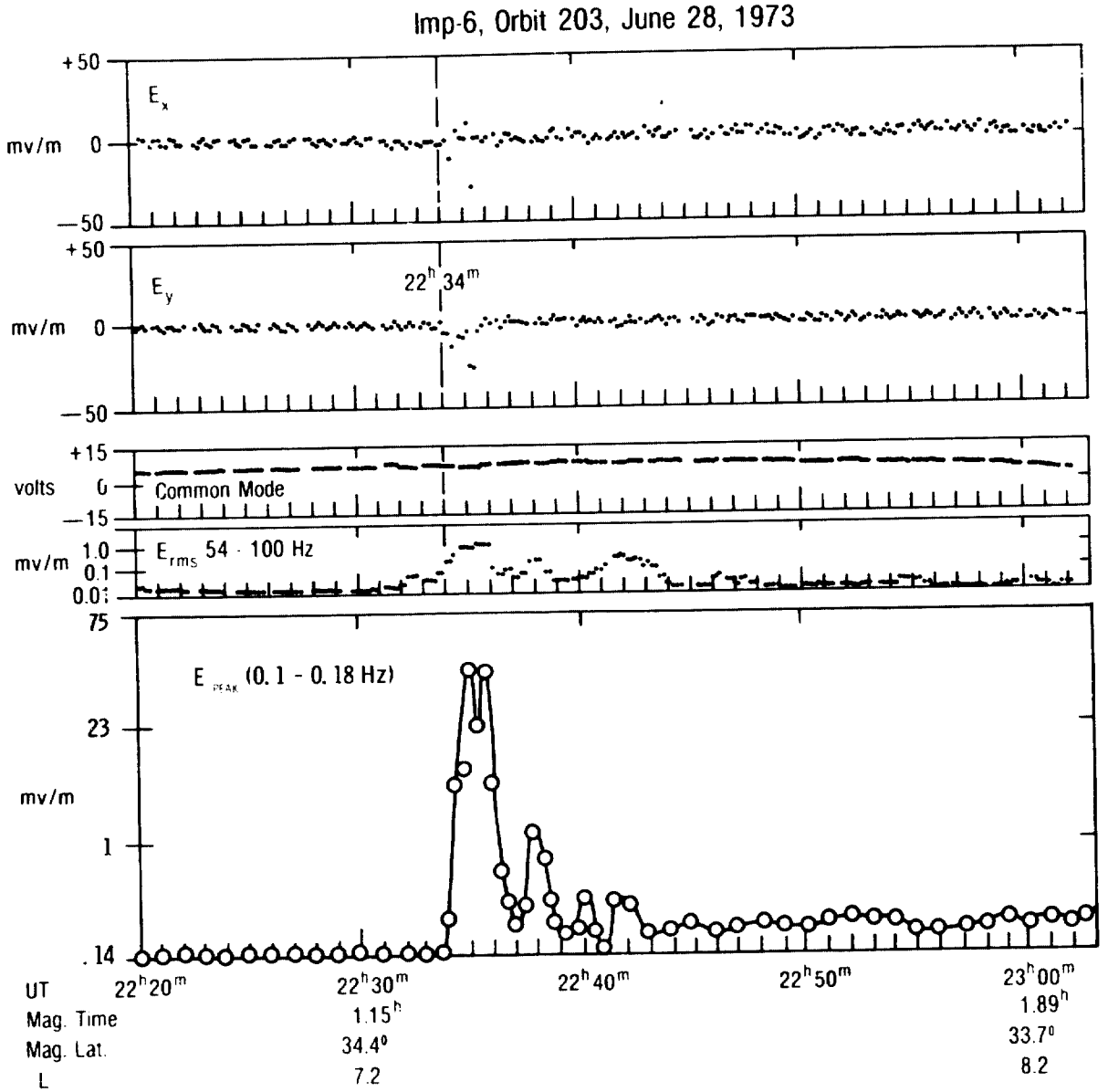
Imp-6, Orbit 203, June 28, 1973
+50
E_x
mv/m 0
−50
+50
E_y
$22^h 34^m$
mv/m 0
−50
+15
volts 0
Common Mode
−15
mv/m 1.0
E_{rms} 54 - 100 Hz
0.1
0.01
75
E_{PEAK} (0.1 - 0.18 Hz)
23
mv/m
1
.14
UT $22^h 20^m$ $22^h 30^m$ $22^h 40^m$ $22^h 50^m$ $23^h 00^m$
Mag. Time 1.15^h 1.89^h
Mag. Lat. 34.4° 33.7°
L 7.2 8.2

FIGURE 1

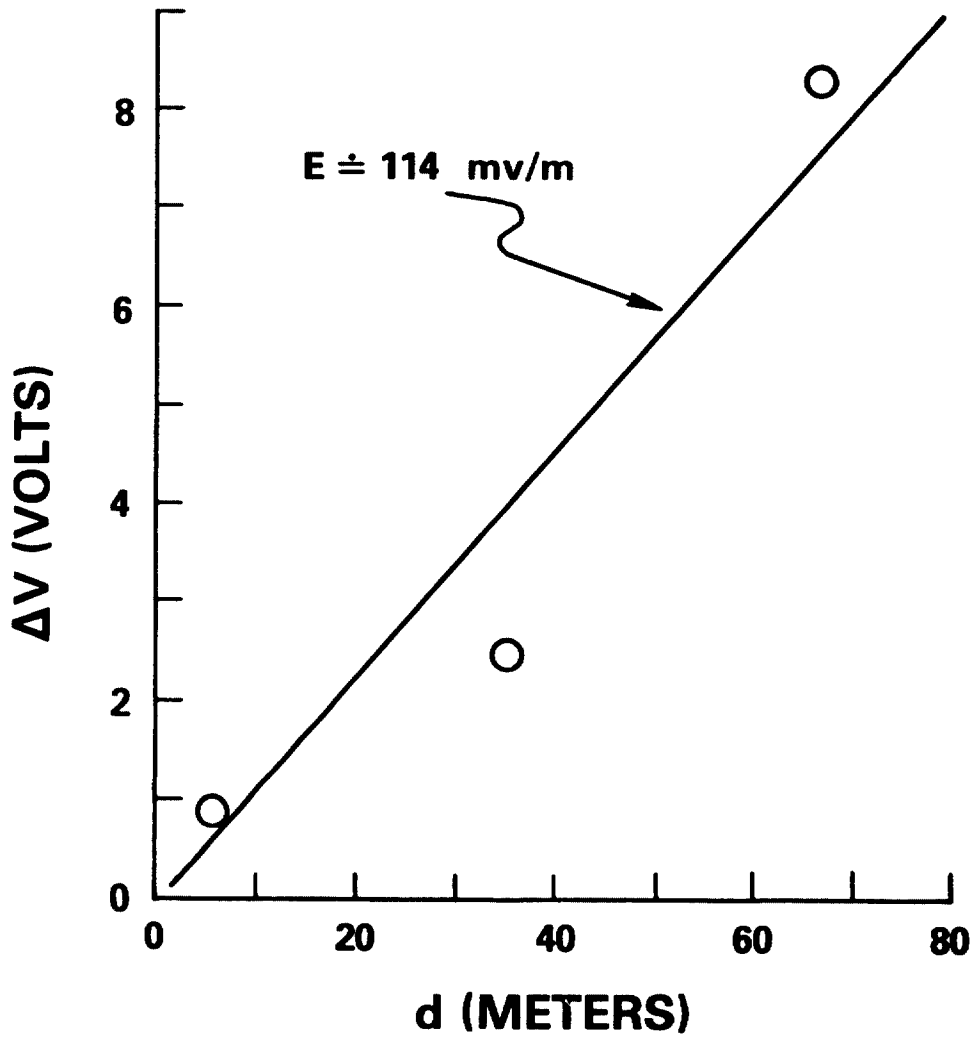

FIGURE 2(a)

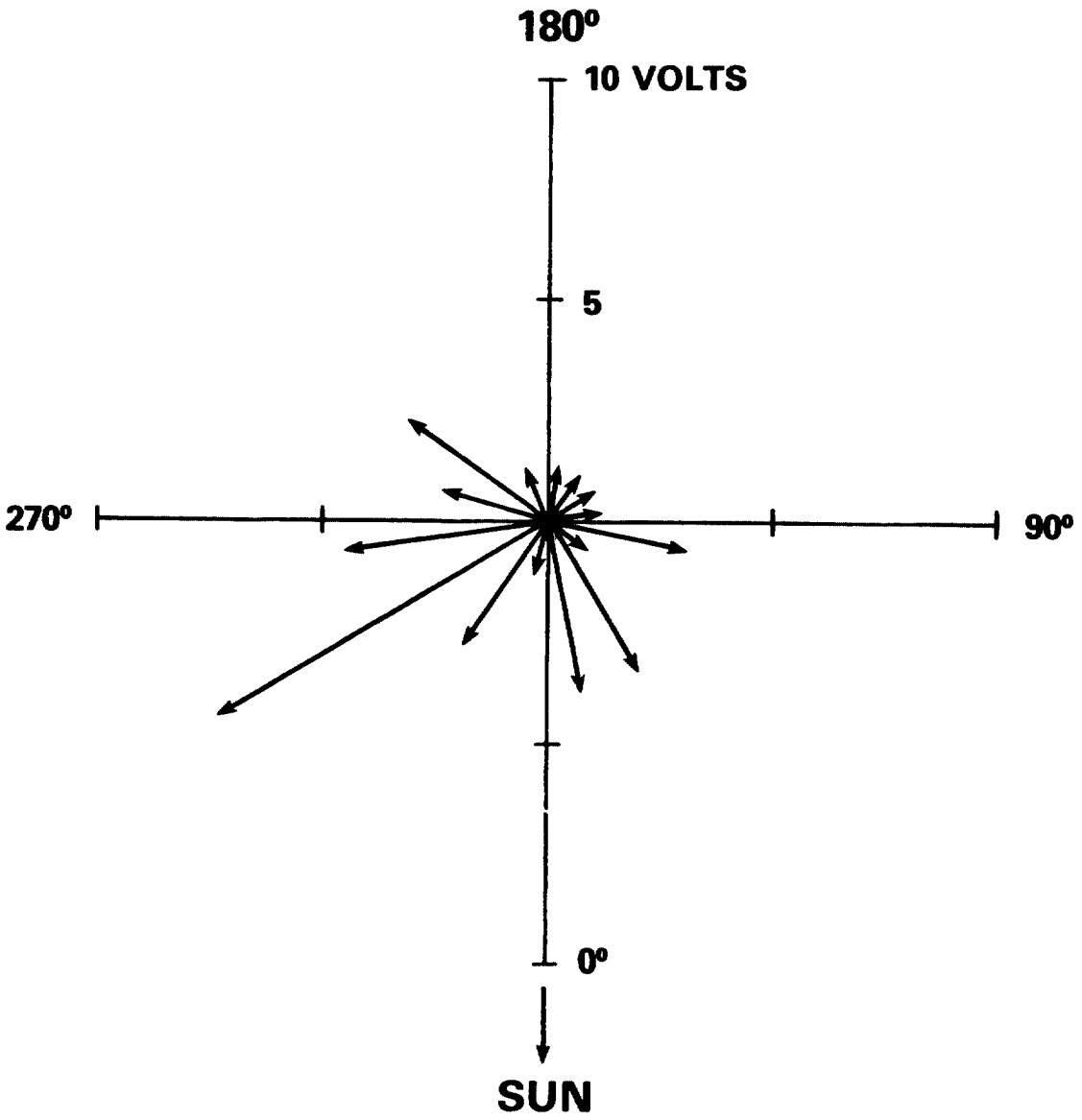

FIGURE 2(b)

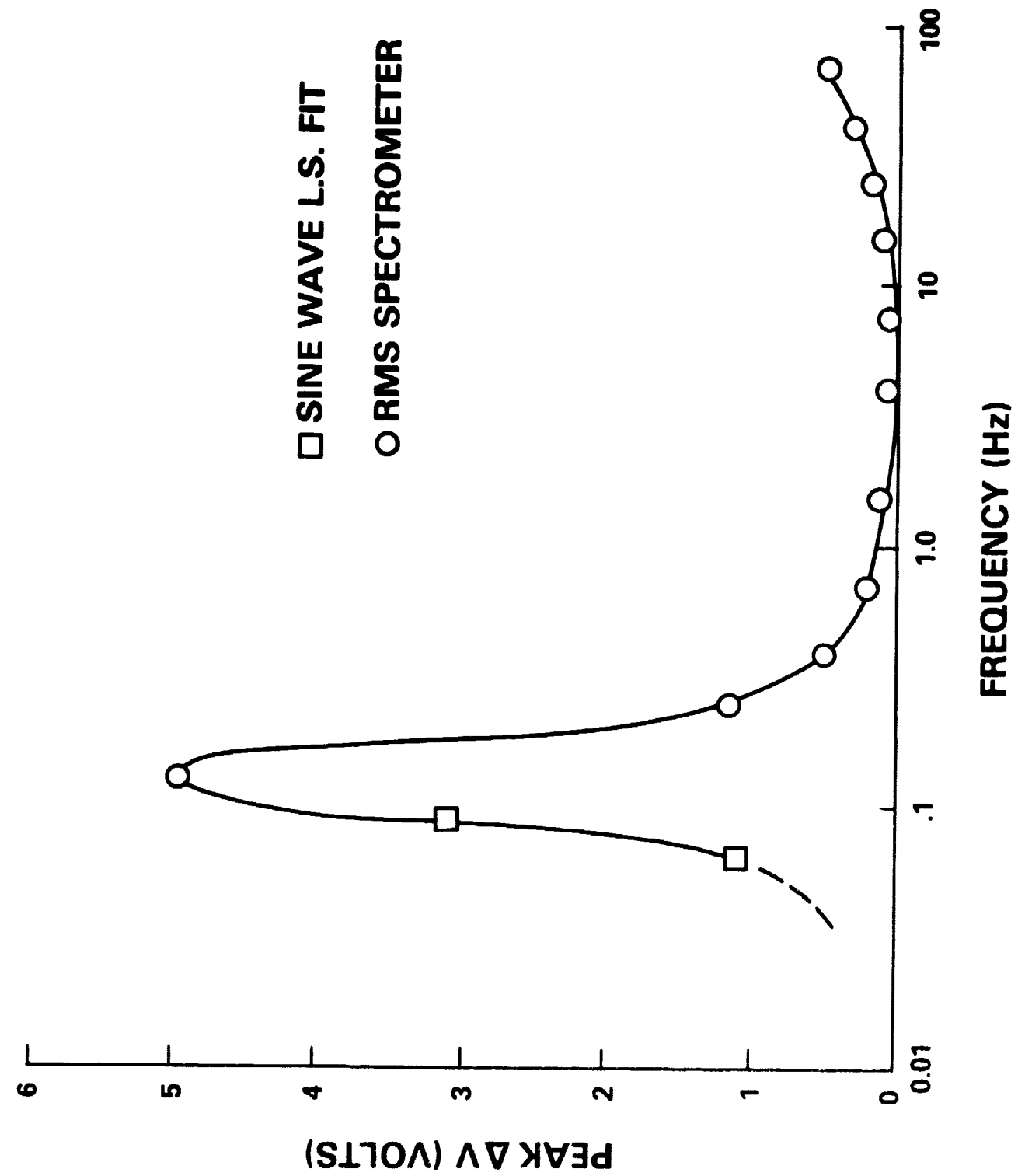
□ SINE WAVE L.S. FIT
○ RMS SPECTROMETER
PEAK ΔV (VOLTS)
FREQUENCY (Hz)
0
1
2
3
4
5
6
0.01
.1
1.0
10
100

FIGURE 3(c)

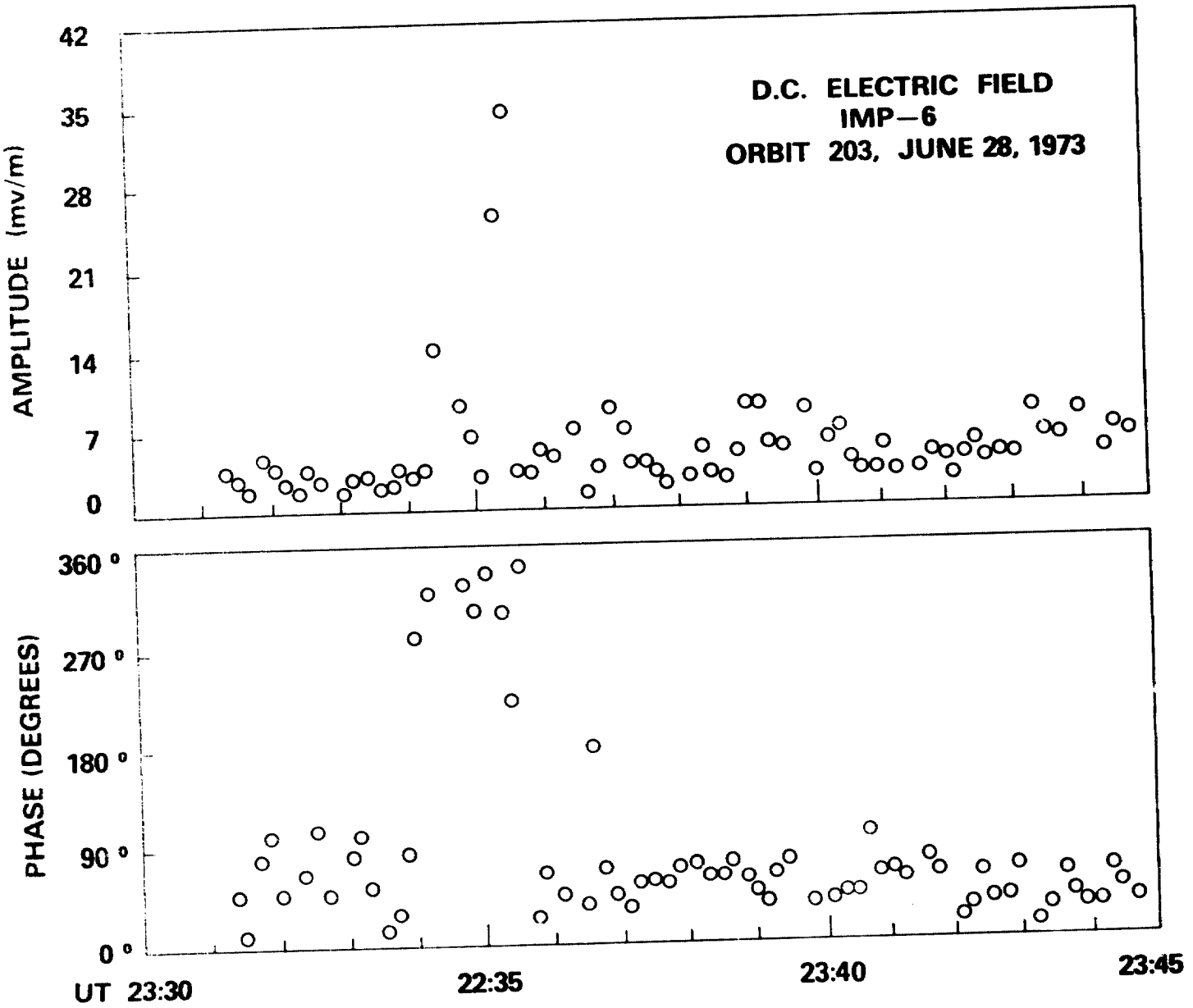
D.C. ELECTRIC FIELD
IMP—6
ORBIT 203, JUNE 28, 1973
AMPLITUDE (mv/m)
42
35
28
21
14
7
0
PHASE (DEGREES)
360 °
270 °
180 °
90 °
0 °
UT 23:30
22:35
23:40
23:45

FIGURE 2(p)

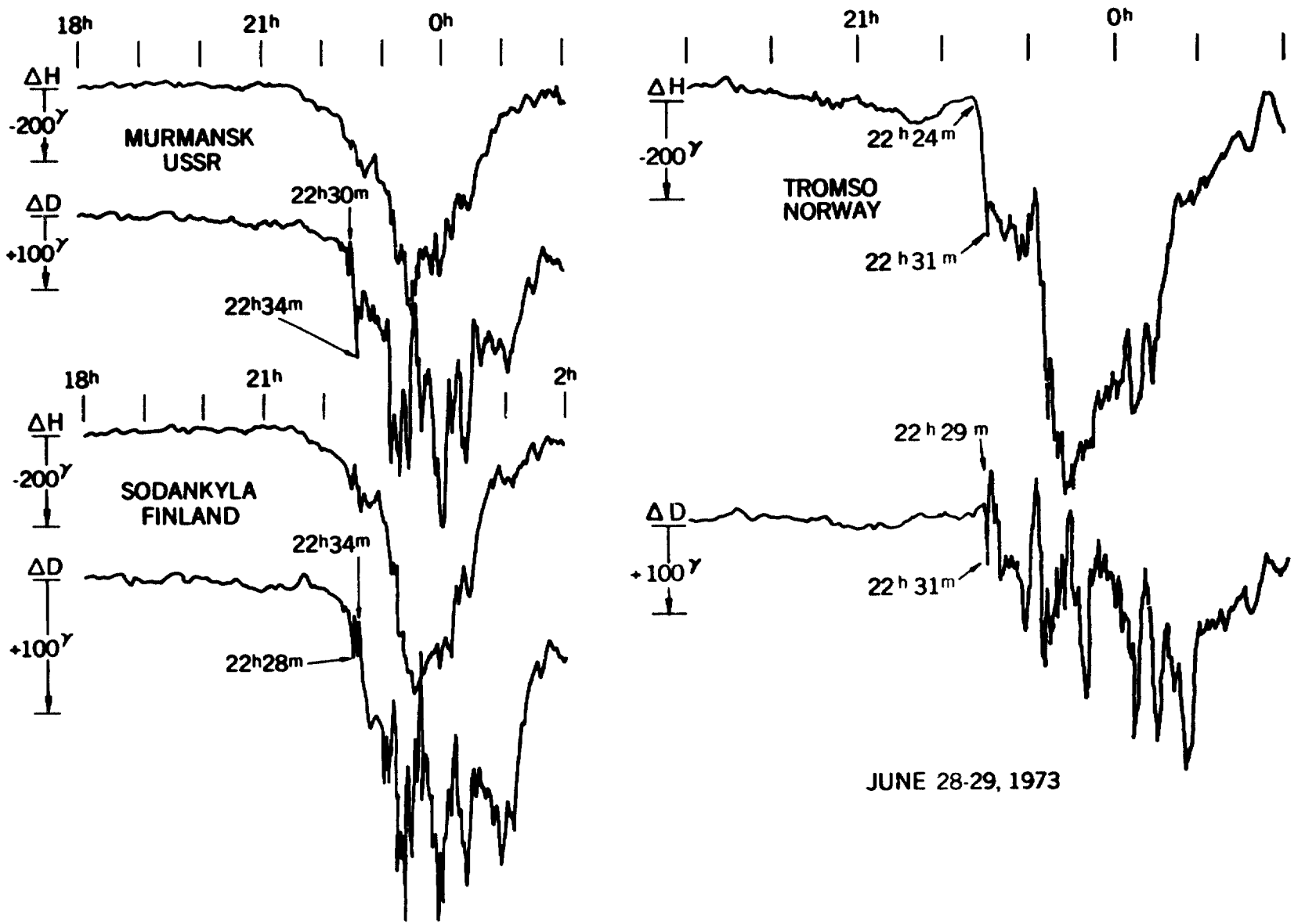
18h
21h
0h
ΔH
-200γ
MURMANSK
USSR
ΔD
+100γ
22h30m
22h34m
18h
21h
2h
ΔH
-200γ
SODANKYLA
FINLAND
22h34m
ΔD
+100γ
22h28m
21h
0h
ΔH
-200γ
22h24m
TROMSO
NORWAY
22h31m
22h29m
ΔD
+100γ
22h31m
JUNE 28-29, 1973

FIGURE 3

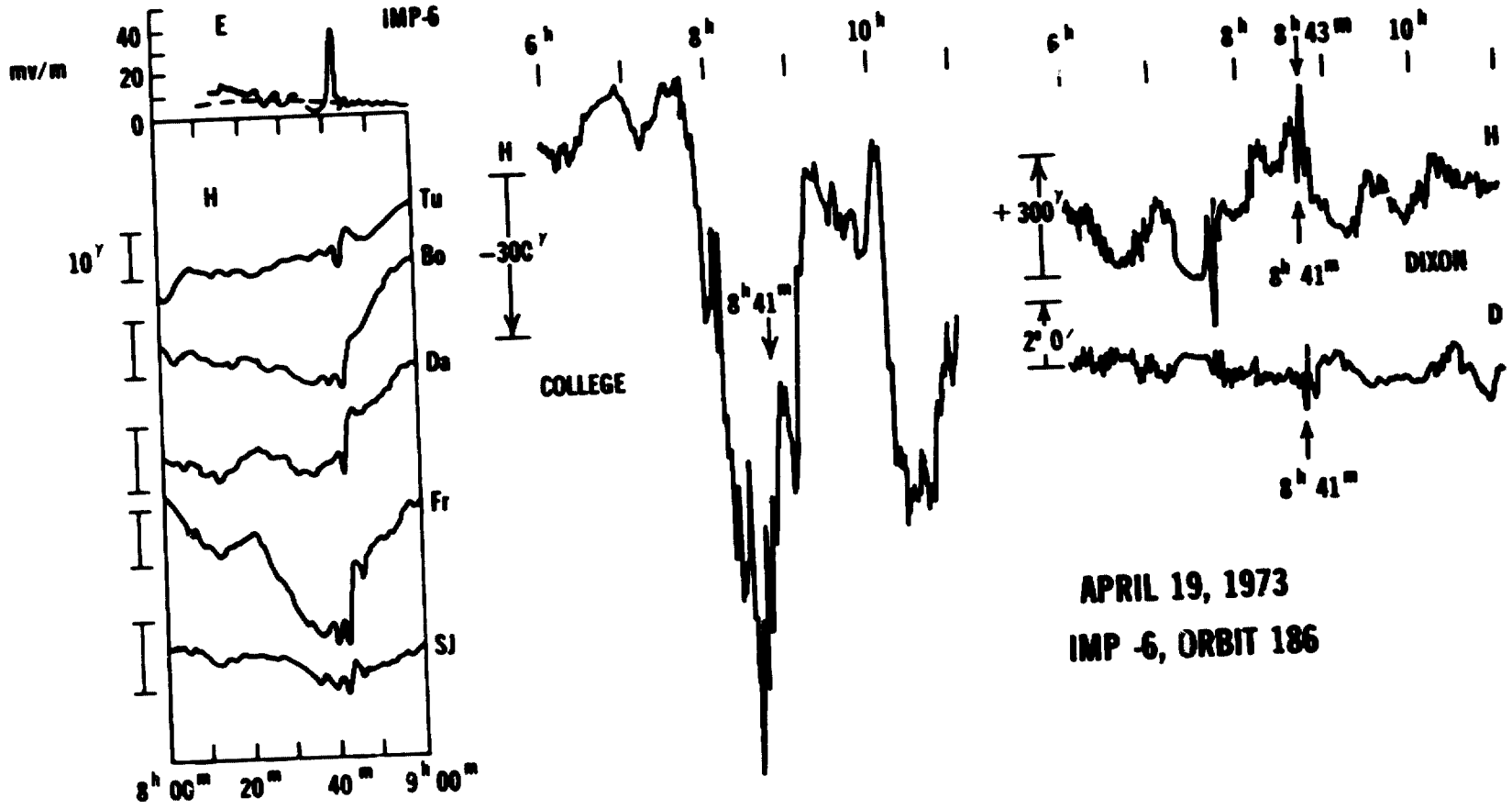
mv/m
40
20
0
E
IMP-6
H
Tu
Bo
Da
Fr
SJ
10γ
8h 00m
20m
40m
9h 00m
6h
8h
10h
H
-300γ
8h 41m
COLLEGE
6h
8h
8h 43m
10h
H
+300γ
8h 41m
DIXON
D
2° 0′
8h 41m
APRIL 19, 1973
IMP -6, ORBIT 186

FIGURE 4

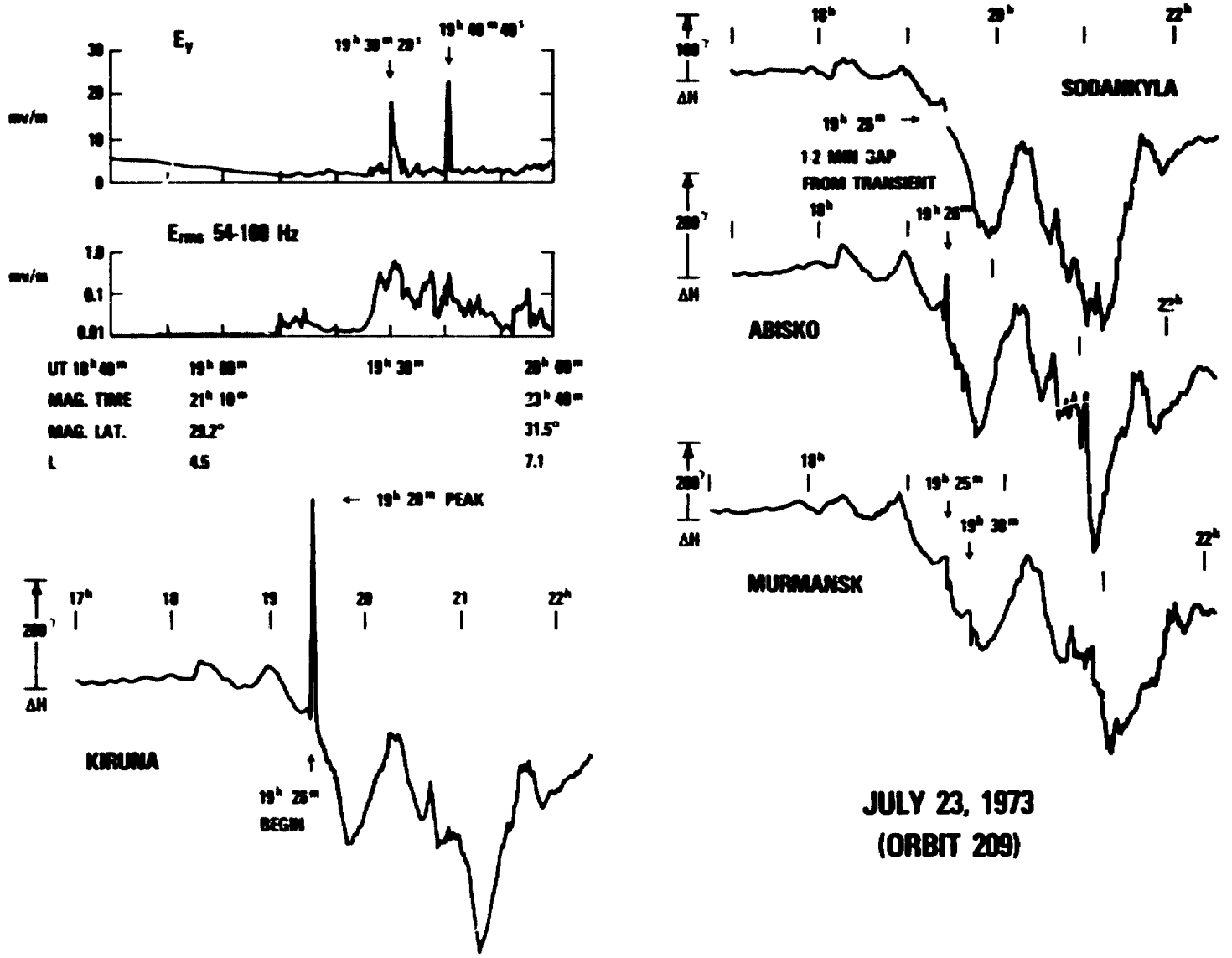
E_y
19h 38m 29s
19h 40m 40s
mv/m
30
20
10
0
E_{rms} 54-180 Hz
mv/m
1.0
0.1
0.01
UT 19h 40m
19h 00m
19h 30m
20h 00m
MAG. TIME
21h 10m
23h 40m
MAG. LAT.
29.2°
31.5°
L
4.5
7.1
← 19h 28m PEAK
17h
18
19
20
21
22h
200γ
ΔH
KIRUNA
19h 25m
BEGIN
18h
20h
22h
100γ
ΔH
SODANKYLA
19h 25m →
12 MIN GAP
FROM TRANSIENT
18h
19h 28m
200γ
ΔH
ABISKO
22h
18h
19h 25m
19h 38m
200γ
ΔH
MURMANSK
22h
JULY 23, 1973
(ORBIT 209)

FIGURE 5

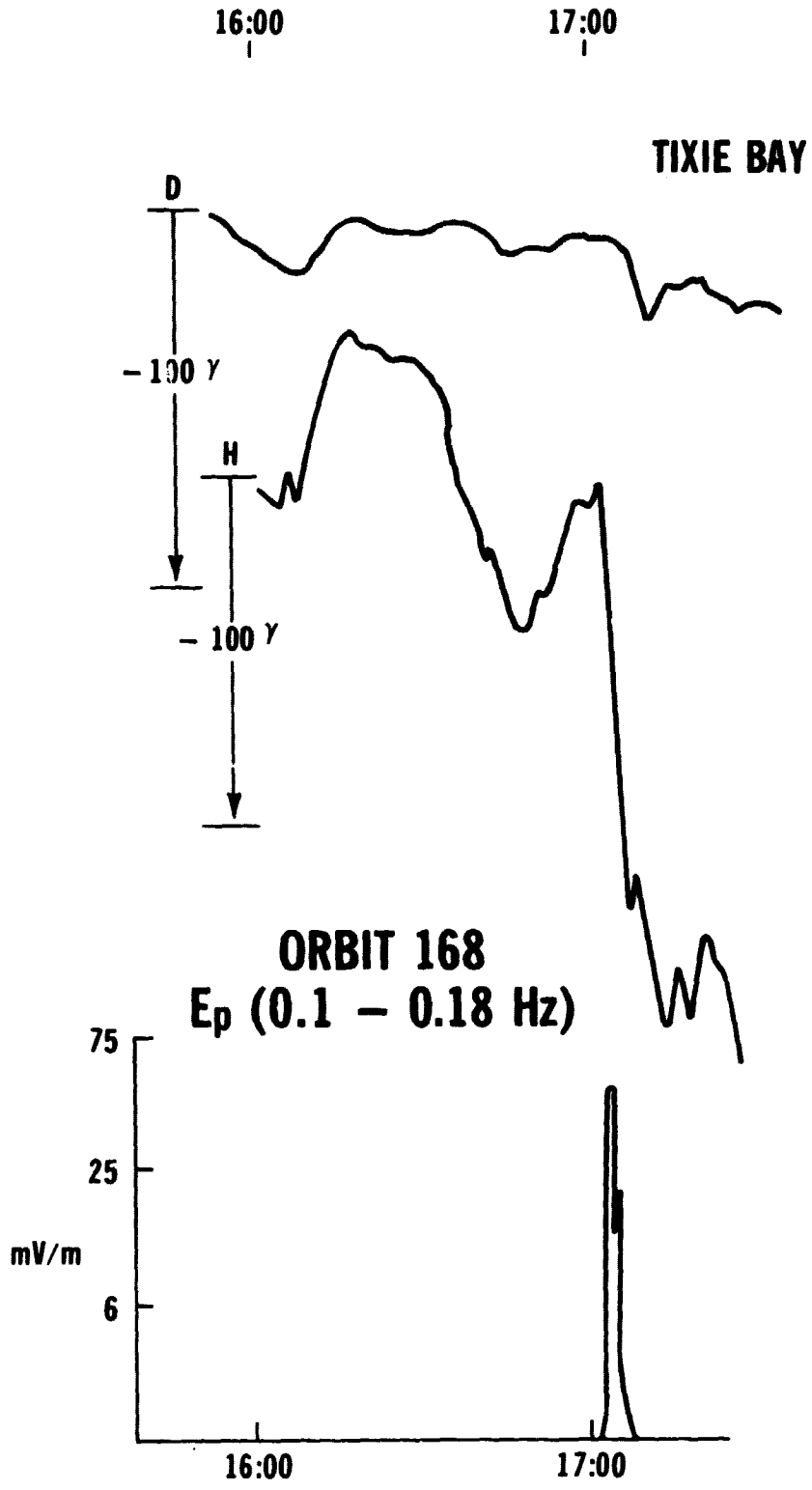
16:00
17:00
TIXIE BAY
D
– 100 γ
H
– 100 γ
ORBIT 168
Ep (0.1 – 0.18 Hz)
75
25
mV/m
6
16:00
17:00
U.T., FEB 7, 1973

FIGURE 6

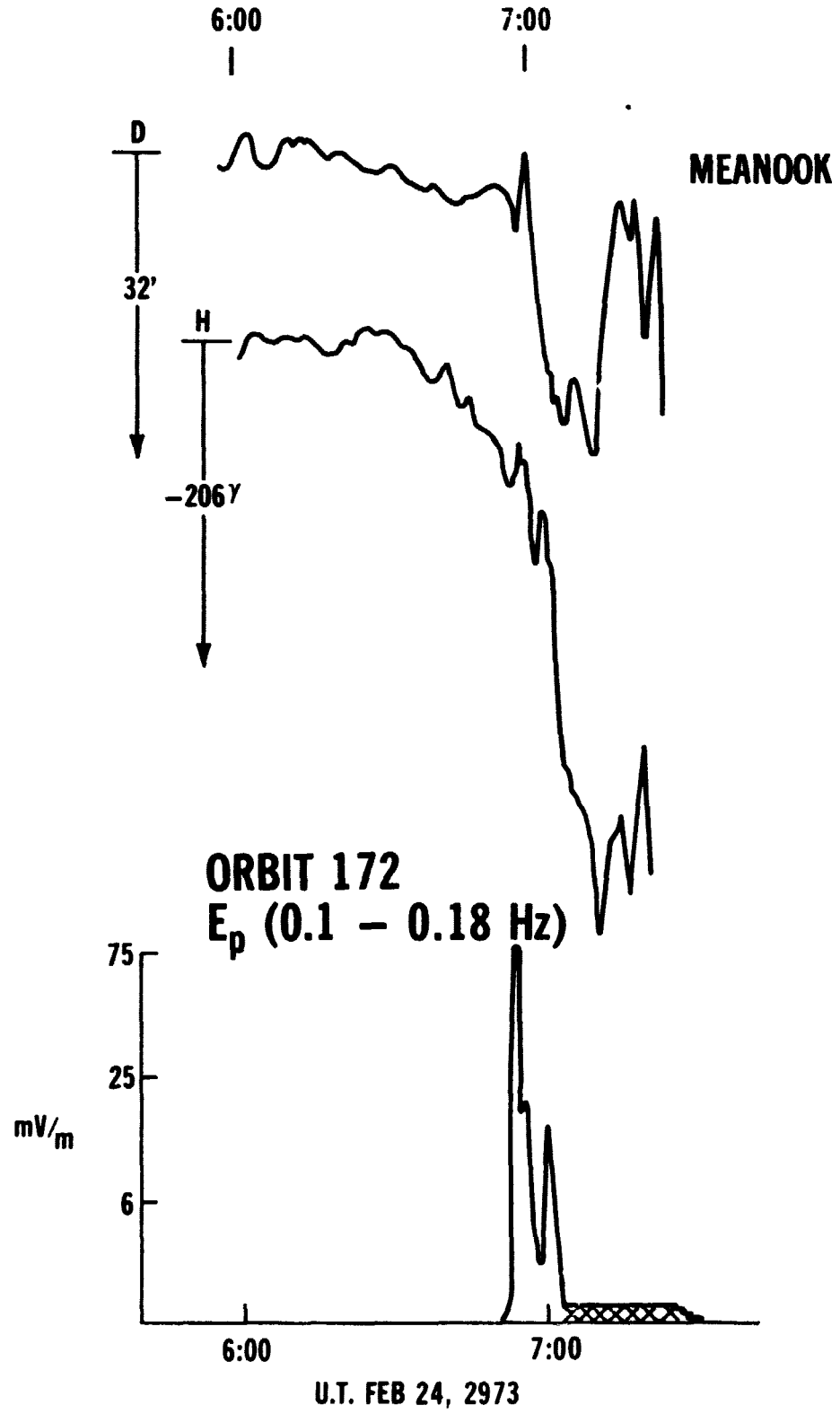
6:00
7:00
D
32'
H
−206γ
MEANOOK
ORBIT 172
E_p (0.1 – 0.18 Hz)
75
25
6
mV/m
6:00
7:00
U.T. FEB 24, 2973

FIGURE 7

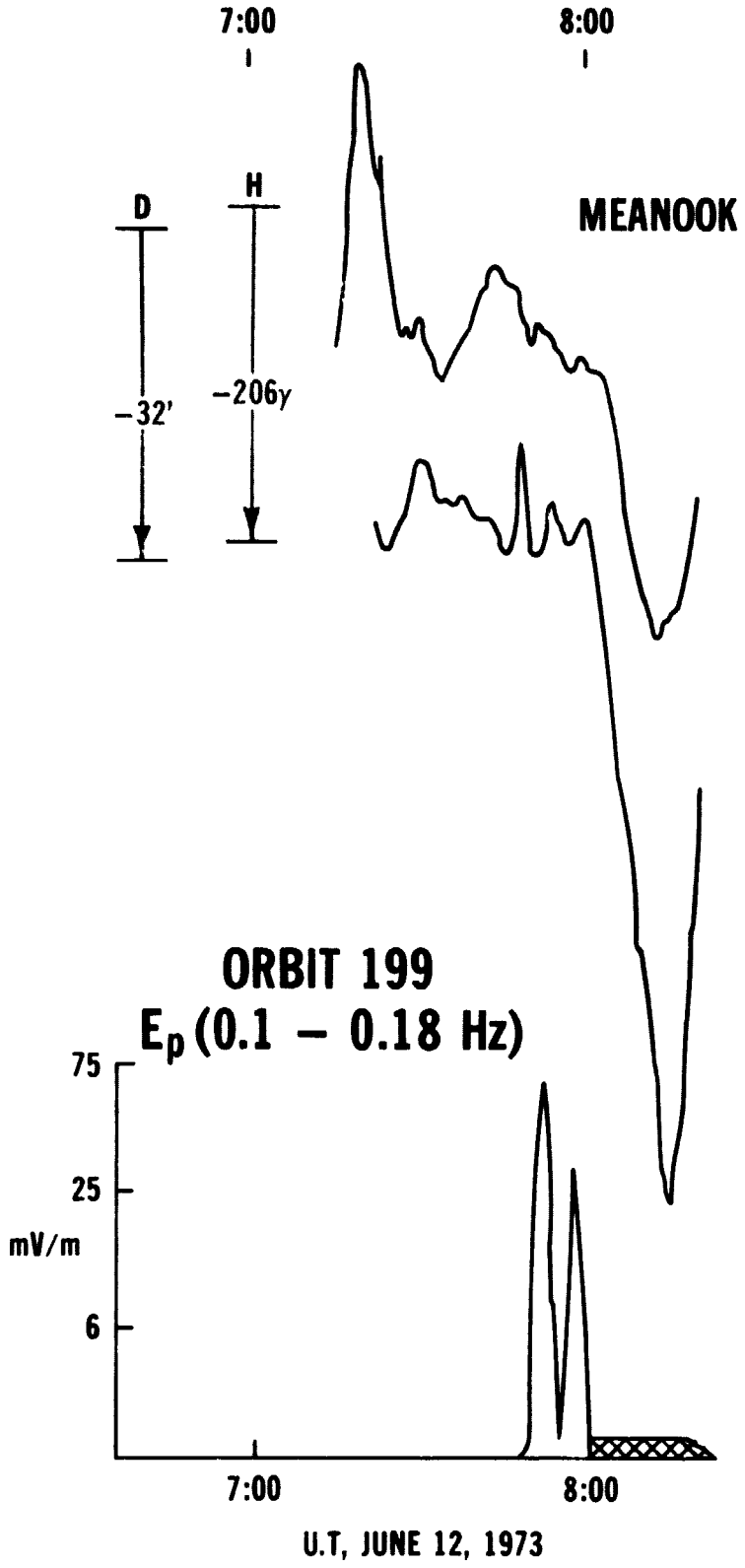
7:00
8:00
D
H
MEANOOK
-32'
-206γ
ORBIT 199
Ep (0.1 – 0.18 Hz)
75
25
mV/m
6
7:00
8:00
U.T, JUNE 12, 1973

FIGURE 8

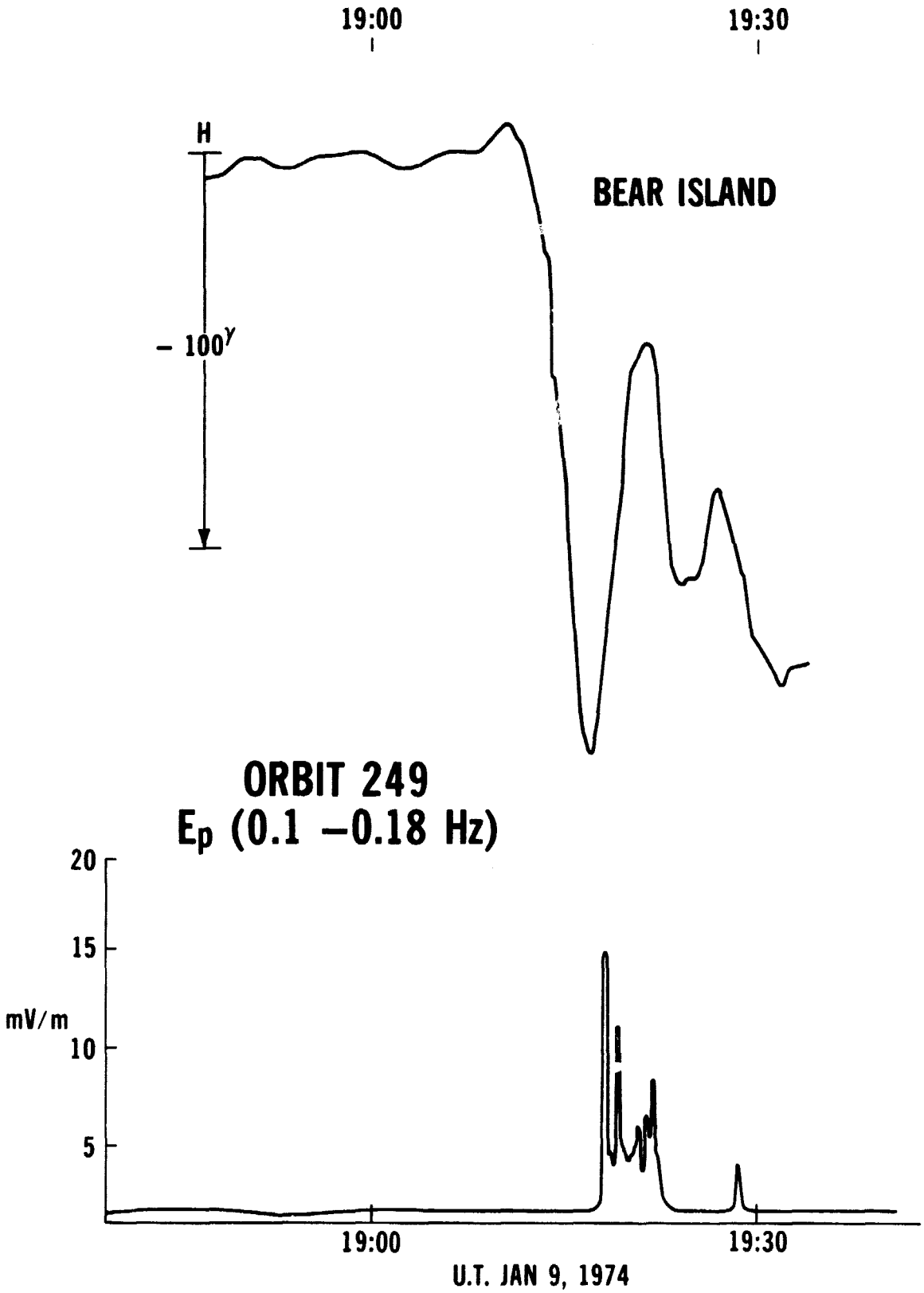
19:00
19:30
H
BEAR ISLAND
– 100γ
ORBIT 249
Ep (0.1 –0.18 Hz)
20
15
mV/m
10
5
19:00
19:30
U.T. JAN 9, 1974

FIGURE 9

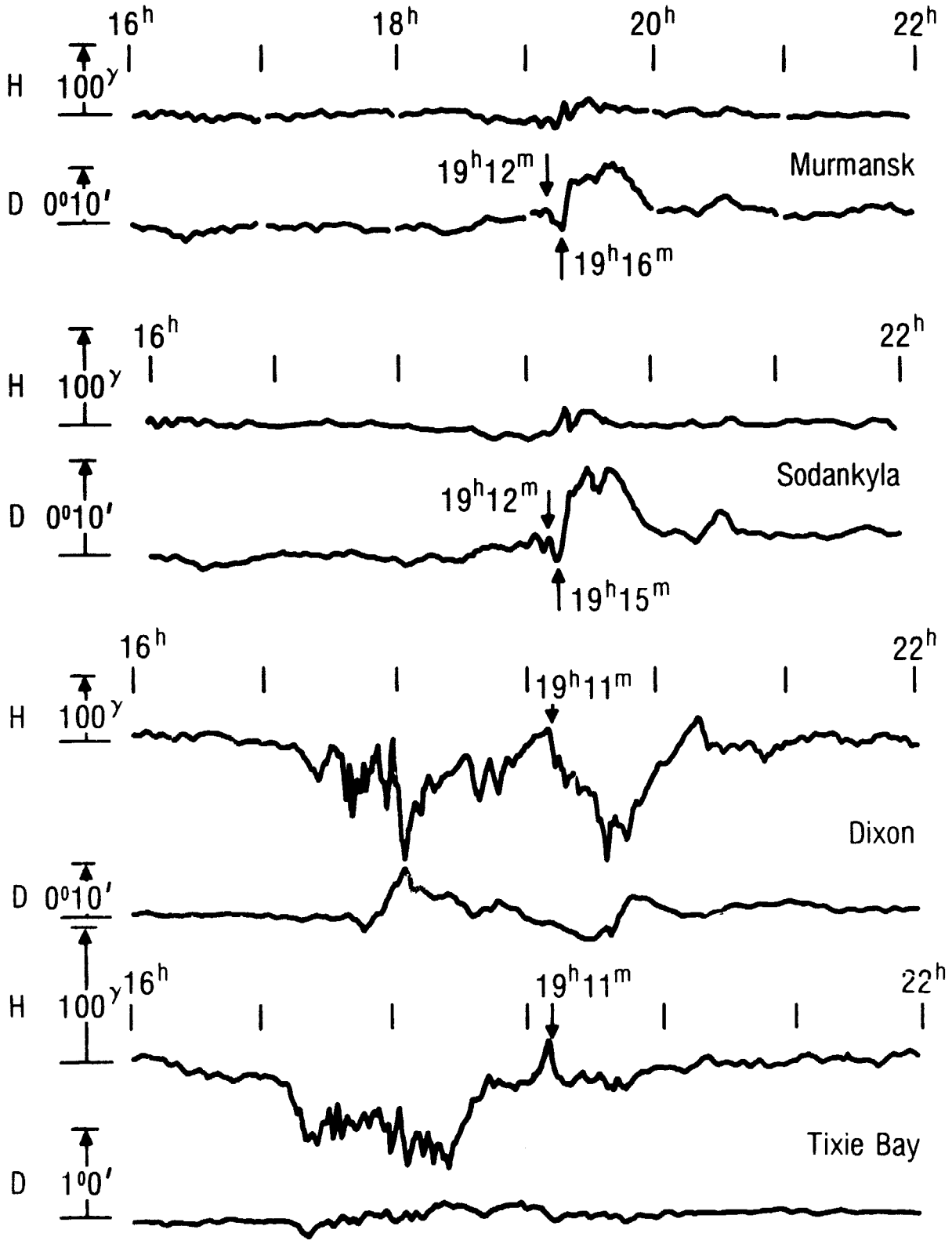
January 9, 1974
16h
18h
20h
22h
H 100γ
D 0°10′
19h12m
19h16m
Murmansk
16h
22h
H 100γ
D 0°10′
19h12m
19h15m
Sodankyla
16h
19h11m
22h
H 100γ
Dixon
D 0°10′
H 100γ
16h
19h11m
22h
Tixie Bay
D 1°0′

FIGURE 10

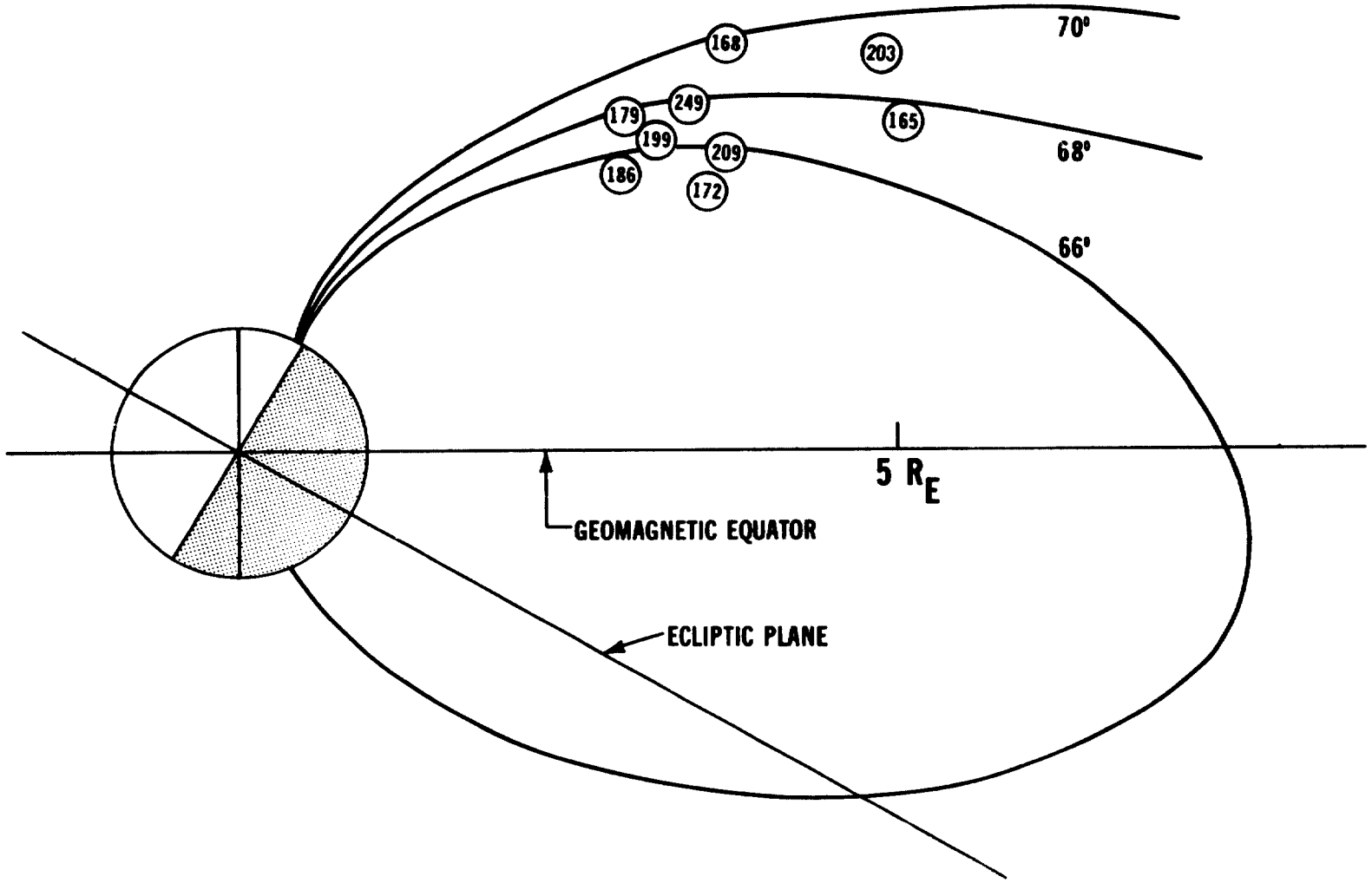
70°
68°
66°
168
203
249
179
165
199
209
186
172
5 R_E
GEOMAGNETIC EQUATOR
ECLIPTIC PLANE

FIGURE 11